



Law of Carrying Cuttings in Horizontal Well Drilling of Marine Natural Gas Hydrate

Na Wei¹(✉), Yang Liu¹, Anqi Liu², Jinzhou Zhao¹, Liehui Zhang¹,
Haitao Li¹, Lin Jiang¹, Zhenjun Cui¹, and Hanming Xu¹

¹ State Key Laboratory of Oil and Gas Reservoir Geology and Exploitation
of Southwest Petroleum University, Chengdu 610500, Sichuan, China
1263839547@qq.com

² Geological Exploration and Development Research Institute of CNPC
Chuanqing Drilling Engineering Co., Ltd., Chengdu 610051, Sichuan, China

Abstract. For rational design of drilling process parameters and guarantee of safe drilling, law of carrying cuttings in horizontal well drilling of marine natural gas hydrate should be intense research to effectively reduce the friction of drilling tools and avoid well blockage. The research was carried out through FLUENT simulation, orthogonal test analysis, rock carrying experiment verification. The critical velocity charts of different hydrate abundance, hydrate-cuttings particle size and drilling fluid density were obtained. Simulation results show that: The critical rock-carrying velocity increases with the increase of the grain size of hydrate-cuttings, decreases with the increase of drilling fluid density, and decreases with the increase of hydrate abundance. Orthogonal test method was used to evaluate the influence of various factors on rock carrying capacity: hydrate-cuttings particle size > hole enlargement way > hydrate abundance > drilling fluid density. The influence of different ways of diameter enlargement on the law of rock carrying is greatly considered in the paper. The research results provide an early technical support for the construction parameter optimization and well control safety of horizontal well exploitation models in marine natural gas hydrate reservoir.

Keywords: Marine natural gas hydrate · Horizontal wells · Fluent · Orthogonal test method · Carrying cuttings capacity · Critical flow velocity

Copyright 2019, IFEDC Organizing Committee

This paper was prepared for presentation at the 2019 International Field Exploration and Development Conference in Xi'an, China, 16–18 October, 2019.

This paper was selected for presentation by the IFEDC Committee following review of information contained in an abstract submitted by the author(s). Contents of the paper, as presented, have not been reviewed by the IFEDC Technical Team and are subject to correction by the author(s). The material does not necessarily reflect any position of the IFEDC Technical Committee its members. Papers presented at the Conference are subject to publication review by Professional Team of IFEDC Technical Committee. Electronic reproduction, distribution, or storage of any part of this paper for commercial purposes without the written consent of IFEDC Organizing Committee is prohibited. Permission to reproduce in print is restricted to an abstract of not more than 300 words; illustrations may not be copied. The abstract must contain conspicuous acknowledgment of IFEDC. Contact email: paper@ifedc.org.

© Springer Nature Singapore Pte Ltd. 2020

J. Lin (Ed.): *Proceedings of the International Field Exploration and Development Conference 2019*, SSGG, pp. 1140–1153, 2020.

https://doi.org/10.1007/978-981-15-2485-1_100

1 Introduction

Natural gas hydrate is a kind of white crystalline clathrate compound formed by hydrocarbon molecules such as methane and water molecules under low temperature and high pressure. It looks like ice and is commonly called “combustible ice” [1, 2]. Natural gas hydrate is characterized by high density, high calorific value and wide distribution and so on [3]. Its carbon content is equivalent to twice the total carbon content of proven fossil energy sources in the world, which can be used as an unconventional and clean energy to replace the global oil and gas [4]. In the 21st century, as a clean energy source, natural gas hydrates is mainly distributed in the terrestrial permafrost and the water depth of 300–3000 m, of which about 90% are stored in deep sea areas [5]. According to incomplete statistics, the total amount of natural gas hydrate resources in the world is about $2.1 \times 10^{16} \text{ m}^3$, while the total amount of natural gas hydrate in China is about $80.1 \times 10^{12} \text{ m}^3$, among which the content of the South China sea, the East China sea, the Qinghai-Tibet Plateau and the Northeast permafrost are $64.2 \times 10^{12} \text{ m}^3$, $3.38 \times 10^{12} \text{ m}^3$, $12.5 \times 10^{12} \text{ m}^3$ and $2.8 \times 10^{12} \text{ m}^3$ respectively [6–8]. Facing such a huge amount of resources, how to efficiently and safely develop marine natural gas hydrates has always been a research hotspot in China and the world.

During the drilling of horizontal wells in the marine gas hydrate layer, hydrate particles and cuttings particles will migrate with the drilling fluid in the horizontal annulus. Due to the gravity, it is easy to deposit in the horizontal section, occurring the accumulation of cuttings, and the cuttings bed will be formed, which is not beneficial to bring up cuttings and results in the decrease of wellbore purification ability. Then the extended capability of the horizontal well will be restricted and the friction torque of the drilling tool will increase, which may cause blockage of the wellbore in severe cases [9–12].

At present, the research on the law of carrying cuttings of conventional oil and gas field drilling has been relatively mature at home and abroad, but there are few studies on the problem of carrying cuttings in the development of deep sea gas hydrate. Therefore, this paper refers to the influence factors of carrying cuttings in the conventional oil and gas field drilling process, using FLUENT simulation technology to simulate the hydrate-carrying capacity of right-angle expansion, 45-degree angle expansion and arc expanding. This paper mainly studies the critical velocity of carrying rock under the condition of different hydrate abundance, hole enlargement way, hydrate-cuttings particle size and drilling fluid density. And the influence order and optimal combination of each influencing factor are determined by orthogonal test analysis method, which provides early technical support for the optimization of operation parameters and well control safety of horizontal well exploitation mode of marine gas hydrate reservoir.

2 Modeling

2.1 Geometric Model

Using Creo2.0 software, the geometric model of the horizontal pipe section with a length of 4.35 m, inner diameter of 0.127 m and outer diameter of 0.216 m is established. The lengths and diameters of right-angle, 45-degree angle and arc expanding section are all 1 m and 0.32 m, respectively, and the expanding ratio is 1.5 times.

The geometric models of the right-angle, 45-degree angle and arc expansion are respectively imported into Meshing in Workbench15.0 for mesh division, and the changes of physical parameters in the boundary region are not taken into account. Among them, the right-angle hole enlargement model partitioning grid number is 869988, node number is 172672; the 45-degree angle hole enlargement model partitioning grid number is 865937, node number is 171835; the grid number of arc expanding is 831509, the number of nodes is 165028. The drilling fluid inlet, outlet, inner wall and outer wall are named respectively. The geometry schematic diagrams of the right-angle, 45-degree angle and arc expansion geometry are shown in Fig. 1.

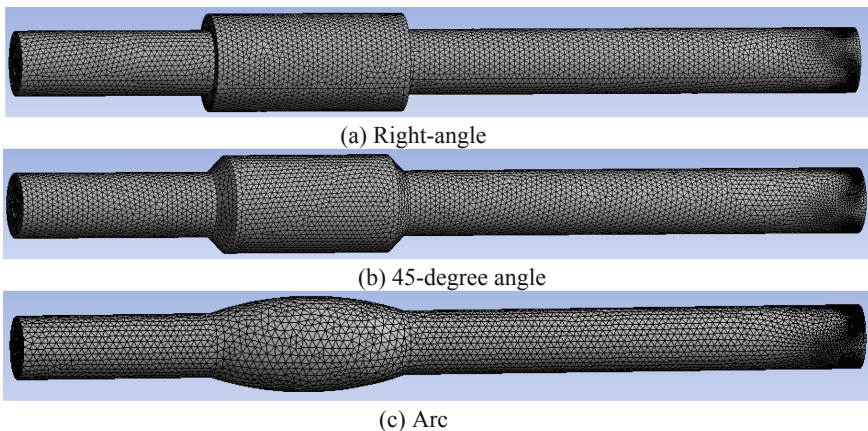


Fig. 1. Schematic diagram of different hole enlargement way model in horizontal section

2.2 Basic Assumptions and Physical Models

The basic assumptions made in the modeling process are as follows:

- (1) The flow process conforms to the continuous medium principle, that is, the hydrate particles are all continuous media.
- (2) The transfer of interphase mass in the hydrate slurry is not considered, that is, the formation and decomposition of hydrate are ignored.
- (3) Ignoring the fluid is a compressible medium.
- (4) The law of conservation of mass, momentum and energy all are satisfied in the flow process of the pipeline.

Based on these basic assumptions, the physical models used are mainly multi-phase flow model and turbulence model.

The multi-phase flow model adopts particle quasi-fluid model, also known as the Euler-Euler model, which is composed of continuity equation, momentum equation, energy equation and fluid composition equation.

Continuity equation:

Gas phase:

$$\frac{\partial}{\partial t}(A\rho_g E_g) + \frac{\partial}{\partial s}(A\rho_g v_g E_g) = q_g - x_g r_H \quad (1)$$

Liquid phase:

$$\frac{\partial}{\partial t}(A\rho_m E_m) + \frac{\partial}{\partial s}(A\rho_m v_m E_m) = -(1 - x_g)r_H \quad (2)$$

Hydrate-cuttings:

$$\frac{\partial}{\partial t}(A\rho_c E_c) + \frac{\partial}{\partial s}(A\rho_c v_c E_c) = q_c \quad (3)$$

Momentum equation:

$$\begin{aligned} \frac{\partial}{\partial t}(AE_g\rho_g v_g + AE_m\rho_m v_m + AE_c\rho_c v_c + AE_H\rho_H v_H) + \frac{\partial}{\partial s}(AE_g\rho_g v_g^2 + AE_m\rho_m v_m^2 \\ + AE_c\rho_c v_c^2 + AE_H\rho_H v_H^2) + Ag \cos \alpha(E_g\rho_g + E_m\rho_m + E_c\rho_c + E_H\rho_H) + \frac{d(Ap)}{ds} + \frac{d(AF_r)}{ds} = 0 \end{aligned} \quad (4)$$

Energy equation:

$$\frac{\partial}{\partial t}(\rho_l E_l (h + \frac{1}{2}v^2 - g \cdot s \cdot \cos \theta))A_t + \frac{\partial(w_l(h + \frac{1}{2}v^2 - g \cdot s \cdot \cos \theta))}{\partial s} = \frac{2}{B'}(T_a - T_t) \quad (5)$$

Fluid composition equation:

$$\frac{\partial}{\partial t}(\rho Y_s) + \frac{\partial}{\partial x_j}(\rho v_j Y_s) = \frac{\partial}{\partial x_j}(\frac{\mu_e}{\sigma_Y} \frac{\partial Y_s}{\partial x_j}) - \omega_s + \alpha_s \sum n_k m_k \quad (6)$$

Where: $\rho_g, \rho_m, \rho_c, \rho_H$ are the density of gas, drilling fluid, cuttings and hydrate, respectively, kg/m^3 ; v_g, v_m, v_c, v_H are the velocity of gas output, drilling fluid and hydrate, respectively, m/s ; q_c is cuttings formation rate, kg/s ; E_g is the volume fraction of the produced gas, dimensionless; A is annulus area, m^2 ; q_g is the decomposition rate of the hydrate layer per unit length, $\text{kg}/(\text{s m})$; x_g is the mass fraction of natural gas in gas hydrates, dimensionless; r_H is the rate of formation of gas hydrate particles per unit

length, kg/(s m); α is hole drift angle, rad; F_r is annulus friction, Pa; p is annulus pressure, Pa. h is enthalpy, it's made up of internal energy and pressure energy; w_l are the mass flow of gas and liquid phase, respectively, kg/s; E_g , E_l are the volume fraction of gas and liquid phase, respectively, dimensionless; T_a , T_t are the temperature of annulus and drill pipe, respectively, °C.

The turbulence model is the standard $k - \varepsilon$ model.

2.3 Parameter Setting and Model Solving

The geometric model was imported into FLUENT to set boundary parameters:

(1) The hydrate density is 950 kg/m^3 , and the cuttings density is 2600 kg/m^3 . (2) It is assumed that the hydrate particle abundance is 10%, 20% and 30% respectively. Then, the corresponding hydrate-debris particle density is calculated as 2435 kg/m^3 , 2270 kg/m^3 and 2105 kg/m^3 by weighted average. As the temperature and pressure change little while moving in the horizontal section, the decomposition amount of the hydrate particles is very small, so the decomposition rate is approximately zero.

Firstly, the geometric model with parameters was imported into FLUENT15.0, and then the coupling interface edem_udf of EDEM2.7 was imported into FLUENT15.0. The k-epsilon model was selected, seawater drilling fluid and methane gas were set in the FLUENT15.0. Among them, the operation steps of EDEM2.7 are:

- (1) Importing the model, setting the material steel and particle.
- (2) Setting the particle diameter to 4 mm, and the particle size was randomly generated according to 1 ± 0.05 times of diameter during simulation.
- (3) Setting the rotational speed of the horizontal segment model to 30 rad/s.
- (4) The virtual area, the area of generating particles, set as four symmetric small circles with a radius of 35 mm.
- (5) Coupling Server coupling switch, click Start to start coupling.

3 The Critical Flow Velocity Plate

3.1 Hydrate Abundance 10% and Particle Size 4 mm

Gas hydrate abundance, particle size, generation speed, rotating speed and bit size are set as 10%, 4 mm, 3000 particle/s, 30 rad/s and 215.9 mm, respectively. After 10 s simulation time, the particle distribution maps of different flow velocities after carrying rock for 10 s are shown in Figs. 3, 4 and 5 respectively.

As indicated in Fig. 2, when the drilling fluid flow rate is 0.8 m/s, a large number of particles are accumulated on the left under right-angle expansion. When the drilling fluid flow rate increase to 0.9 m/s, the particles piled on the left side have been significantly reduced. When its rate reaches to 1 m/s, the number of particles packing is basically the same as that of particles at 0.9 m/s.



Fig. 2. Particle distribution map after 10 s simulation time with different velocity under right-angle expansion

In Fig. 3 when the drilling fluid flow rate is 0.6 m/s, large quantities of particles are accumulated on the left under 45-degree angle expansion. However, the particle has been significantly reduced by at half while the drilling fluid flow rate rise to 0.7 m/s, and the particle situation of 0.7 m/s are the basically same as 0.8 m/s. Compared with the right-angle expansion, the 45° angle is more inclined than the right-angle, the cuttings particles more easily from escaping from the 45° angle hole enlargement section.



Fig. 3. Particle distribution map after 10 s simulation time with different velocity under 45-degree angle expansion

In Fig. 4, when the drilling fluid flow rate is 0.3 m/s, large quantities of particles are accumulated on the left under arc expansion. When the drilling fluid flow rate increase to 0.4 m/s, the volume of the left part is greatly reduced. When its rate reaches to 1 m/s, there is substantially no particle accumulation at arc expansion section.

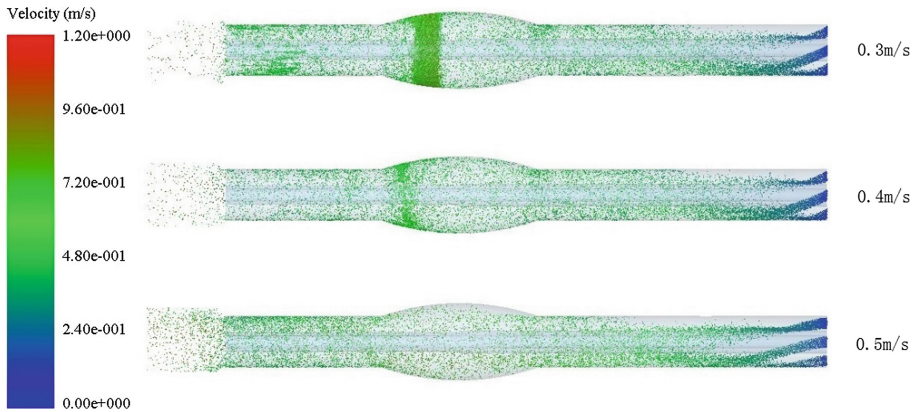


Fig. 4. Particle distribution map after 10 s simulation time with different velocity under arc expansion

Therefore, the critical rock-carrying flow velocity of drilling fluid for the right-angle expansion, 45-degree angle expansion and arc expansion are 0.9 m/s, 0.7 m/s and 0.4 m/s respectively.

3.2 Different Hydrate Abundance and Particle Size

The four particle sizes of 2 mm, 4 mm, 6 mm and 8 mm are respectively simulated under the condition of the hydrate abundance of 10%, 20% and 30%, that is, each hydrate abundance value should be simulated for the corresponding four particle sizes. The critical flow velocity plate could be obtained as shown in Fig. 5.

It can be seen from Fig. 5 that in the three hole enlargement way, the critical flow velocity for carrying cuttings increases with the increase of the particle size of the hydrate-rock debris when the hydrate abundance is constant; the critical flow rate decreases with the increase of hydrate abundance when the particle size of the hydrate-rock debris is constant. When the hydrate abundance and the particle size of the hydrate-rock debris are both constant, the carrying cuttings capacity in right-angle expansion method is the poorest, the carrying cuttings capacity in 45-degree angle expansion method is medium, and the carrying cuttings capacity in arc expanding method is the best. The reasons for this phenomenon are as follows: (1) Because of the increase of hydrate abundance, the density of cuttings decreases and the critical velocity of carrying rock decreases. (2) As the particle size increases, the ability to

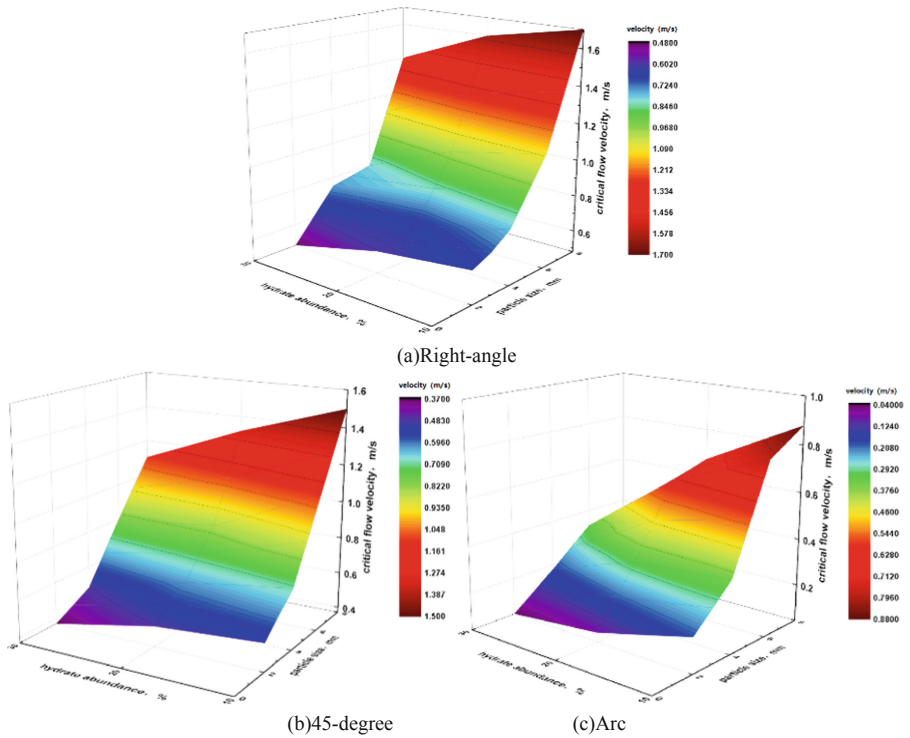


Fig. 5. The critical flow velocity plate of different hydrate abundance and particle size under different hole enlargement way

jump again decreases after collision between particles and pipe wall, and between particles and pipe wall. The increase of particle size also increases its gravity, and the drag force of the drilling fluid carrying particles increases, therefore the critical flow velocity is increased in the expansion section.

3.3 Different Hydrate Abundance and Drilling Fluid Density

The four drilling fluid density of 1030 kg/m^3 , 1130 kg/m^3 , 1230 kg/m^3 and 1330 kg/m^3 are respectively simulated under the condition of the hydrate abundance of 10%, 20% and 30%, that is, each hydrate abundance value should be simulated for the corresponding four drilling fluid density. The critical flow velocity plate could be obtained as shown in Fig. 6 under three different hole enlargement way.

It can be seen from Fig. 6 that in the three different hole enlargement way, the critical flow velocity for carrying cuttings decreases with the increase of the drilling fluid density when the hydrate abundance is constant; the critical flow rate decreases with the increase of hydrate abundance when the density of the drilling fluid is constant. When the hydrate abundance and drilling fluid density are both constant, the carrying cuttings capacity in right-angle expansion method is the poorest, the carrying

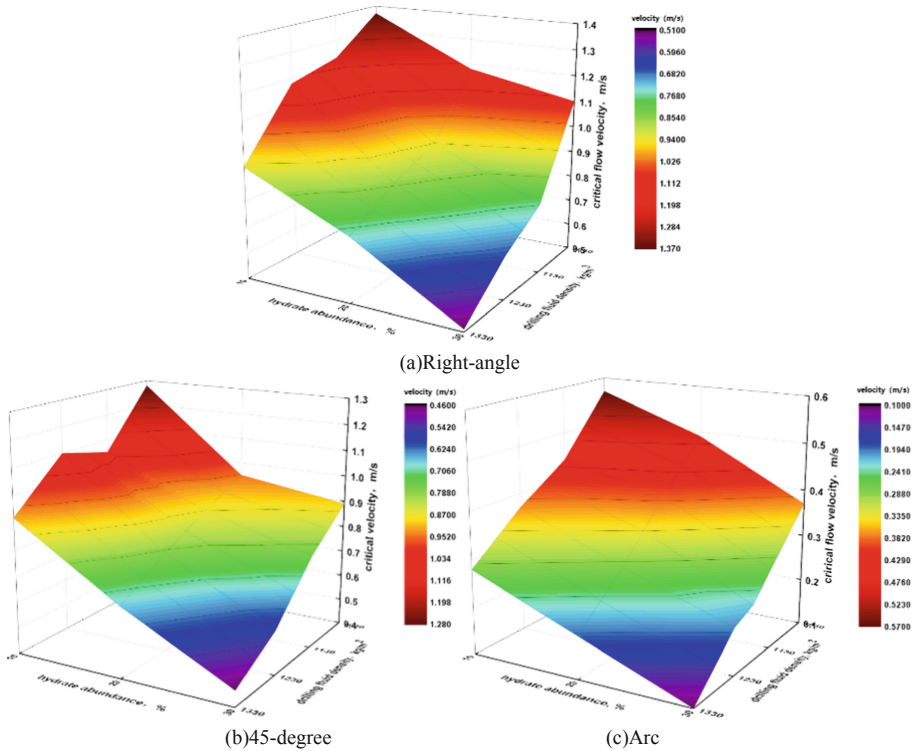


Fig. 6. The critical flow velocity plate of different hydrate abundance and drilling fluid density under different hole enlargement way

cuttings capacity in 45-degree angle expansion method is medium, and the carrying cuttings capacity in arc expanding method is the best. The reasons for this phenomenon are as follows: (1) Because of the increase of hydrate abundance, the density of cuttings decreases and the critical velocity of carrying rock decreases. (2) As the drilling fluid density increases, the drag force of the drilling fluid carrying particles increases, therefore the critical flow velocity is increased in the expansion section.

4 Orthogonal Test Analysis

Orthogonal test method is a method to study multi-factor and multi-level problem. The influence level of each factor can be determined by the statistical analysis of experimental results by orthogonal test method. The orthogonal test method can comprehensively analyze the influence of various factors on rock carrying capacity, and the influence magnitude can be sorted to get the best combination.

In this orthogonal test, four experimental factors are selected, which are expansion mode, hydrate-cuttings particle size, hydrate abundance and drilling fluid density, and three levels are selected for each factor. The critical velocity of carrying rock is taken as

the test index. Under the horizontal wells drilling in marine gas hydrates, the factors influencing of the rock carrying capacity are shown in Table 1 and the results of the analysis are shown in Table 2.

Table 1. Factors influencing and levels of rock carrying capacity

Factors		Levels		
		1	2	3
Expansion mode	(A)	Right-angle	45-degree angle	Arc
Hydrate abundance	(B)	10%	20%	30%
Hydrate-cuttings particle size	(C)	2	4	6
Drilling fluid density	(D)	1030	1130	1230

Table 2. Results of orthogonal test analysis on rock carrying capacity

Case	Factors				Test index
	A	B	C	D	Critical flow velocity m/s
1	Right-angle	10%	2	1030	0.9
2	Right-angle	20%	4	1130	1
3	Right-angle	30%	6	1230	1
4	45-degree	10%	4	1230	0.7
5	45-degree	20%	6	1030	1.1
6	45-degree	30%	2	1130	0.5
7	Arc	10%	6	1130	0.9
8	Arc	20%	2	1230	0.1
9	Arc	30%	4	1030	0.4
K_1	2.9	2.5	1.5	2.4	
K_2	2.3	2.2	1.2	2.4	
K_3	1.4	1.9	3	1.8	
k_1	0.967	0.833	0.500	0.800	
k_2	0.767	0.733	0.400	0.800	
k_3	0.467	0.633	1.000	0.600	
R	0.5	0.2	0.6	0.2	

As shown in Table 2, the test results of no. 8 $A_3B_2C_1D_3$ showed the minimum critical velocity (0.1 m/s), which was the best of all the 9 tests. This is the optimal level combination selected from the experiment. Hydrate-cuttings particle size is the most important factors influencing of horizontal wells drilling in marine gas hydrate, which should be considered in practical operation. The order of the four factors is: hydrate-cuttings particle size > expansion mode > hydrate abundance > drilling fluid density. The optimal combination under the simulated working condition is: arc expansion, hydrate abundance 20%, hydrate-cuttings particle size 2 mm, drilling fluid density 1230 kg/m³.

Since the orthogonal test is only 1/9 all the 3^4 , 81 experiments, it is necessary to verify whether $A_3B_2C_1D_3$ is optimal by using the trend chart of the influence of various factors on critical flow velocity of carrying rock.

In order to judge intuitively, the factors influencing are used as the abscissa, the average value of the index as the ordinate according to the data in Table 2, which draws the trend chart of the influence of various factors on critical flow velocity of carrying rock, as shown in Fig. 7. When comparing K_i values, the minimum K_i level is taken as the optimal level. Among them, K_i is the sum of indicators and data of repeated tests at all levels; k_i is the average of the indicators.

In the influence trend chart, the magnitude of the rise and fall of the horizontal change point indicate the influence degree of this factor on the critical velocity of carrying rock. As shown in Fig. 7, hydrate-cuttings particle size has changed radically, which shows that hydrate-cuttings particle size plays a major role in influencing the critical rock-carrying velocity; the change range of expansion mode is also large, followed by the influence. The order of the four factors is: hydrate-cuttings particle size > expansion mode > hydrate abundance > drilling fluid density, which is consistent with the quantitative discussion results of the above test.

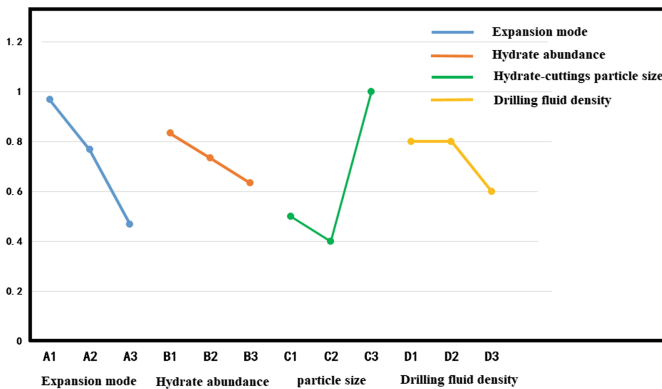


Fig. 7. The trend chart of the influence of various factors on critical flow velocity of carrying rock

5 Experimental Simulation Verification

In order to further verify the accuracy of simulation, referring to Experimental research on horizontal circulation pipeline of hydrate slurry by my experimental team [13, 14], the law of carrying cuttings in horizontal well drilling of marine natural gas hydrate was obtained.

Since the whole experimental device has only arc section, only the experimental results and numerical simulation results of rock carrying in the arc section are verified.

5.1 Experimental Research on Horizontal Circulation Pipeline of Hydrate Slurry

In the experimental research on horizontal circulation pipeline of hydrate slurry, the displacement of governor pump gear is gradually increased from 0, and the solid phase particle migration in the horizontal pipeline is monitored in real time. Then, recording the displacement of solid particles at the critical start-up, the experimental data under different solid particle sizes and different hydrate volume fractions are shown in Tables 3 and 4, respectively.

Table 3. The experimental data under different solid particle sizes

Solid particle sizes, mm	Hydrate volume fractions in solid particle, %	The displacement of solid particles at the critical start-up, L/s	The velocity of solid particles at the critical start-up, m/s	The simulation velocity of solid particles at the critical start-up, m/s
2	16	0.96	0.211	0.181
5	16	1.20	0.263	0.283
8	16	1.87	0.410	0.290
10	16	1.94	0.425	0.440

Table 4. The experimental data under different hydrate volume fractions

Solid particle sizes, mm	Hydrate volume fractions in solid particle, %	The displacement of solid particles at the critical start-up, L/s	The velocity of solid particles at the critical start-up, m/s	The simulation velocity of solid particles at the critical start-up, m/s
5	16	1.2	0.263	0.285
5	32	1.19	0.261	0.250
5	48	1.05	0.230	0.213
5	64	0.68	0.149	0.175

5.2 Comparisons of Simulation with Experiment

By comparing the experimental data with the numerical simulation, the experimental and theoretical correlation curve of the critical start-up velocity under different solid particle sizes and different hydrate volume fractions are shown in Fig. 8.

It can be seen from Fig. 8, with the increase of solid particle size, the critical starting flow velocity increases. The numerical simulation results are consistent with the experimental results that the error is less than 9.62%. With the increase of volume fraction of hydrate in solid particles, the critical starting flow velocity decreases. The numerical simulation results are consistent with the experimental results that the error is less than 8.52%. By comparing the numerical simulation with the experiment, the accuracy of the establishment of the critical flow velocity plate of marine gas hydrate is verified.

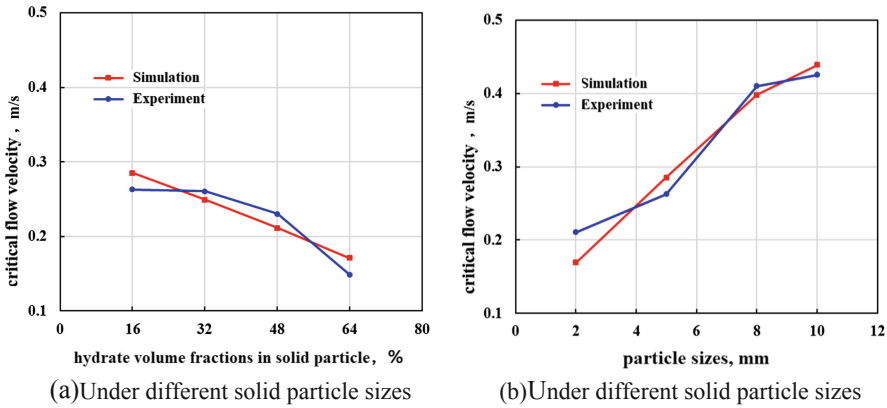


Fig. 8. The experimental and theoretical curves of the critical velocity of particles

6 Conclusions

- (1) This paper establishes three different hole enlargement way models: right-angle expansion method, 45-degree angle expansion method, and arc expanding method. And coupling simulations with EDEM and FLUENT are carried out to obtain the critical flow velocity plate required in the carrying cutting.
- (2) In the three different expansion methods, the critical flow velocity required for carrying cuttings increases with the increase of the particle size of the hydrate-rock debris when the hydrate abundance is constant, and the critical flow velocity required for carrying cuttings decreases with the increase of drilling fluid density, the critical flow rate required for carrying cuttings decreases with the increase of hydrate abundance when the density of the drilling fluid is constant.
- (3) According to the analysis of orthogonal test, the order of the factors influencing the carrying capacity is as follows: hydrate-cuttings particle size > expansion mode > hydrate abundance > drilling fluid density.
- (4) Compared with the experimental results, the numerical simulation results are consistent with the experimental result, the accuracy of the establishment of the critical flow velocity plate of Marine gas hydrate is verified.

Acknowledgments. This research was funded by National Key Research and Development Programs (2016YFC0304008 and 2018YFC0310203), Strategic Research Program of Chinese Academy of Engineering in Science and Technology Medium and Long-Term Development Strategy Research Field (2017-ZCQ-5), Natural Science Foundation of China (51874252), Open Fund Project of State Key Laboratory of Oil and Gas Reservoir Geology and Exploitation (PLN201816), and Scientific Research Starting Project of Southwest Petroleum University (2018QHZ007).

References

1. Feng, J.-C., Li, X.-S., Li, G., et al.: Numerical investigation of hydrate dissociation performance in the South China sea with different horizontal well configurations. *Energies* **7**(8), 4813–4834 (2018)
2. Liu, B., Yuan, Q., Su, K.-H., et al.: Experimental simulation of the exploitation of natural gas hydrate. *Energies* **5**(2), 1–28 (2012)
3. Wei, N., Sun, W., Meng, Y., et al.: Sensitivity analysis of multiphase flow in annulus during drilling of marine natural gas hydrate reservoirs. *J. Nat. Gas Sci. Eng.* **36**, 692–707 (2016)
4. Kezirian, M.T., Phoenix, S.L., et al.: Natural gas hydrate as a storage mechanism for safe, sustainable and economical production from offshore petroleum reserves. *Energies* **10**(6), 1–8 (2017)
5. Wei, N., Sun, W., Meng, Y., et al.: Analysis of decomposition for structure I methane hydrate by molecular dynamic simulation. *Russian J. Phys. Chem. A* **92**(5), 840–846 (2018)
6. Zhou, S., Chen, W., Li, Q., Zhou, J., Shi, H.: Research on the solid fluidization well testing and production for shallow non-diagenetic natural gas hydrate in deep water area. *China Offshore Oil Gas* **29**(4), 1–8 (2017)
7. Zhao, J., Zhou, S., Zhang, L., Wu, K., Guo, P., Li, Q., et al.: The first global physical simulation experimental systems for the exploitation of marine natural gas hydrates through solid fluidization. *Nat. Gas. Ind.* **37**(9), 15–22 (2017)
8. Wei, N., Xu, C., Meng, Y., et al.: Numerical simulation of gas-liquid two-phase flow in wellbore based on drift flux model. *Appl. Math. Comput.* **338**, 175–191 (2018)
9. De Silva, J.M., Dawe, R.: Towards commercial gas production from hydrate deposits. *Energies* **4**(2), 1–24 (2011)
10. Wei, N., Meng, Y., Gao, L., et al.: Cuttings transport models and experimental visualization of underbalanced horizontal drilling. *Math. Probl. Eng.* **10**(2), 1024–1230 (2013)
11. Li, Y., Bjorndalen, N., Kuru, E.: Numerical modelling of cuttings transport in horizontal wells using conventional drilling fluids. *J. Can. Pet. Technol.* **46**(7), 103–107 (2013)
12. Wei, N., Meng, Y., Li, G., et al.: Cuttings-carried theories and erosive energy laws in annular in gas drilling horizontal well. *Thermal Sci.* **18**(5), 1695–1698 (2014)
13. Zhao, J., Li, H., Zhang, L., et al.: Large-scale physical simulation experiment of solid fluidization exploitation of marine gas hydrate. *Nat. Gas. Ind.* **10**(38), 76–83 (2018)
14. Li, S., Wei, N., Li, H., et al.: Migration characteristics of solid-phase particles in horizontal pipes in the exploitation of marine gas hydrate reservoirs through solid fluidization. *Nat. Gas. Ind.* **10**(38), 100–106 (2018)